Magnetic Phase in the Near-Surface Region of an $FeBO_3$ Single Crystal

B. Stahl,[1] E. Kankeleit,[2] R. Gellert,[2] M. Müller,[1] and A. Kamzin[3]

[1]*Fachbereich Materialwissenschaft, Fachgebiet Dünne Schichten, Petersenstrasse 23, TU Darmstadt, D-64287 Darmstadt, Germany*
[2]*Institut für Kernphysik, TU Darmstadt, Schlossgartenstrasse 9, D-64289 Darmstadt, Germany*
[3]*Laboratory of Magnetism, A.F. Ioffe Physical-Technical Institute, Politekhnicheskaya 26, St. Petersburg, 194021, Russia*
(Received 22 October 1999)

An $FeBO_3$ single crystal was studied from 291 K up to the Néel temperature $T_N = 348.35$ K by depth selective conversion electron Mössbauer spectroscopy in ultrahigh vacuum (10^{-9} mbar). A new magnetic near-surface phase was found. Its thickness D diverges on approaching T_N and gives a critical exponent for the correlation length of $\nu = 0.59(4)$. The phase boundary between the bulk and near-surface phase could be identified.

PACS numbers: 75.30.Pd, 75.40.−s, 76.60.Es, 76.80.+y

Surface magnetism has been extensively studied on ultrafine particles [1] as well as on thin films [2]. Pioneering work on ultrafine hematite particles was published by van der Kraan [3] and Shinjo *et al.* [4]. It revealed a different magnetic behavior of the first monolayers with respect to bulk samples. The first depth selective conversion electron Mössbauer spectroscopy (DCEMS) experiment on a polycrystalline hematite film at room temperature [5] gave a thickness of the magnetically distinct near-surface region of 1.8 nm. For theoretical aspects of surface magnetism, see [6].

In experiments on ultrafine particles and thin films not only the presence of a surface or interface may change the magnetic behavior, but also structural differences may play an important role. To avoid such complications, in our experiment the surface of a perfect single crystal was chosen as the most simple geometrical and physical situation possible. The experimental method had thus to fulfill not only the requirements concerning magnetic characterization but should also give an appropriate depth resolution for a variable surface layer of 1 to 100 nm. An ideal tool for studying magnetism is the Mössbauer technique. The improvements in the combination of Mössbauer and conversion electron spectroscopy [7,8] made such a depth resolved experiment feasible. DCEMS makes use of the energy loss of primarily monoenergetic conversion and Auger electrons that are emitted in succession to the Mössbauer absorption process in the sample. This can be used in a deconvolution procedure to get the depth information of the Mössbauer absorption [9].

The $FeBO_3$ single crystal (enriched to 96% in ^{57}Fe) was prepared by the flux method and subsequently cleared of its surface by mechanical and chemical polishing. Thus a structural homogeneous sample was obtained. This is confirmed by the detailed DCEMS analysis of the isomer shift and quadrupole splitting in the paramagnetic state. The root mean square of the surface roughness was measured by atomic-force microscopy in a 500 nm by 500 nm area to give 0.4 nm. The c axis of the single crystal is oriented perpendicularly to the surface and the local magnetic moments of the canted antiferromagnet.

As our DCEMS experiment on a hematite single crystal at room temperature [10] confirmed the finding of Ref. [5], we focused our experimental investigation on the temperature dependence of the near-surface magnetic properties of an $FeBO_3$ single crystal, which has a similar magnetic structure as hematite. The first investigations of this kind were realized by Kamzin *et al.* [11] by comparing the Mössbauer signal detected by transmitted γ quanta, backscattered x rays, and conversion electrons. Apart from a depth dependent gradual change of the magnetic structure in a surface region, a continuous reduction of the Néel temperature by approaching the surface was proposed. In the work of Kovalenko *et al.* [12] relaxation effects have been found in a near-surface layer. The crude depth resolution in the above experiments ($\approx$100 nm) did not allow for an unambiguous characterization of the near-surface magnetic behavior.

The present study gives results for a surface region of 600 nm in thickness with an appropriate resolution. The main finding is the coexistence of a homogeneous magnetic near-surface phase and the antiferromagnetic bulk phase. Both are separated by a phase boundary that is unambiguously identified by its hyperfine interaction. The near-surface phase is characterized by strong relaxation effects that include a paramagnetic contribution down to 0.65 K below T_N. Near-surface and transition phases show a systematic dependence of their thickness as a function of temperature.

To get an idea of the temperature dependent differences of the magnetic ordering as a function of depth in the crystal, Fig. 1 shows the Mössbauer spectra for two electron energy settings of the orange spectrometer [7] at the K conversion edge of ^{57}Fe. The respective depth weight functions are showing the surface sensitivity for 7.25 keV and a rather flat distribution for 6.50 keV. All spectra are normalized to equal area and the residuals between the two columns are shown. At 341.25 K the Mössbauer spectra can be mainly understood by a reduction of the average magnetic hyperfine field in a surface layer. By approaching T_N, in addition, the near-surface spectrum shows the characteristics of a fast (10^{-8} s) relaxation. This is similar

 0031-9007/00/84(24)/5632(4)$15.00

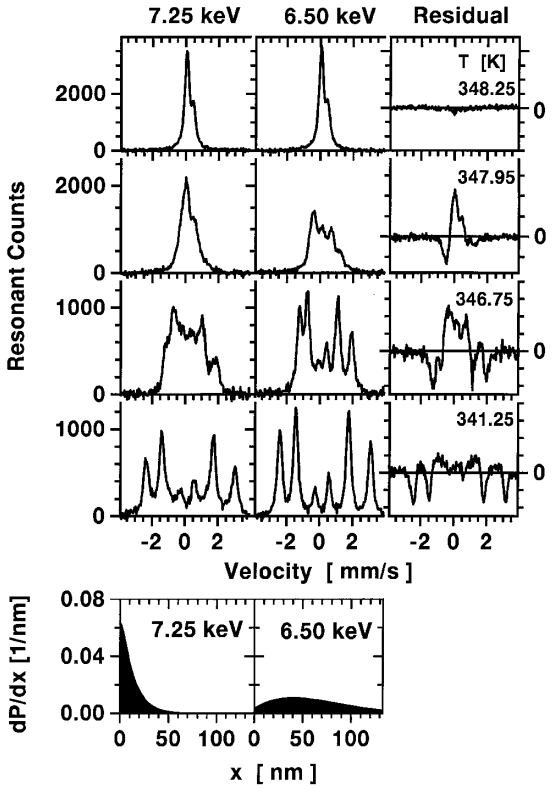

FIG. 1. Mössbauer spectra for two electron energies and the corresponding depth weight functions. The residuals have the same scales as the Mössbauer spectra.

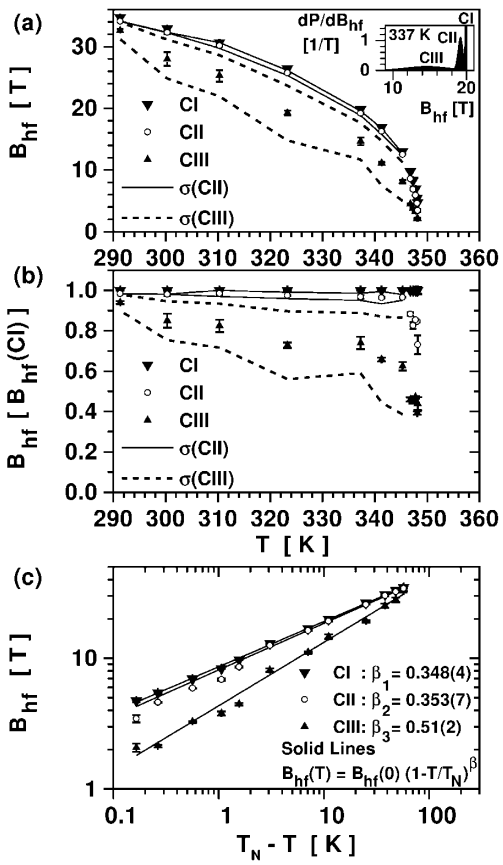

FIG. 2. Magnetic hyperfine field of CI–CIII as a function of temperature. (a) Symbols represent the average of B_{hf} for each component; lines indicate the sigma value of the Gaussian distribution. The inset shows the distribution at 337 K. (b) B_{hf} in units of B_{hf}(CI). (c) Logarithmic plot of B_{hf} versus t.

to superparamagnetic behavior but is caused by spin wave excitations at lower temperatures and critical fluctuations in the vicinity of T_N. From the intensity ratio of the Mössbauer lines it can be concluded that the relaxation takes place perpendicularly to the crystallographic c-axis.

At 348.25 K, just 0.1 K below T_N, the two Mössbauer spectra in Fig. 1 look almost identical. This is a clear indication that the thickness of the magnetically distinct surface region has grown to about 200 nm. The L conversion electrons of ^{57}Fe allow the determination of this thickness, as their weight functions cover a 600 nm surface region.

By analyzing the temperature and electron energy dependence of the Mössbauer spectra, a deconvolution into three components CI–CIII could be established: CI exhibits the same characteristics as bulk $FeBO_3$ [13], CII is similar to CI but shows a small reduction and distribution of the magnetic hyperfine field, and CIII shows a reduction of the average hyperfine field by 15% already at 300 K in combination with a wide hyperfine field distribution with a standard deviation of 10%. It turns out that the paramagnetic contribution in the Mössbauer spectra for reduced temperatures $t = T_N - T$ of 0 K $< t <$ 0.65 K is an inherent feature of the near-surface phase CIII and will be named CIIIb. In this context, the magnetically split fraction of component CIII will be named CIIIa.

The temperature dependence of these components is plotted in Fig. 2a. The inset gives the magnetic hyperfine field distribution at 337 K, which is typical for spectra below 346 K. The deconvolution into three distinct magnetic phases is supported by the depth analysis of the DCEMS data. Other deconvolutions that are possible within the statistical error of the Mössbauer spectra, especially for $T >$ 346 K, lead to resonant electron spectra that are not compatible with the electron transport theory. Thus, the depth deconvolution provides additional information that restricts the interpretation of the otherwise partly ambiguous Mössbauer spectra near the Néel temperature. In Fig. 2b the magnetic hyperfine fields are plotted in units of the splitting of component CI. It becomes obvious that CII stays within a constant distance from CI up to temperatures of 346 K. The magnetic hyperfine field shows only a narrow distribution (solid lines). These properties are due to the exchange coupling of phase CII to the spin system of the bulk phase CI. In contrast, CIII shows a stronger collapse of the average magnetic hyperfine field as a function of temperature accompanied by a wide distribution. The logarithmic plot of Fig. 2c reveals the characteristic exponents which are identical for CI and CII within the statistical error bars. The small deviations above 346 K may be due to the statistical correlation of CII with

CIII. The exponent $\beta_1 = 0.348(4)$ is in agreement with Ref. [13]. The stronger decrease with temperature for CIII is given by $\beta_3 = 0.51(2)$, following the same analytical relationship.

The depth information of the above Mössbauer deconvolution is given by the resonant electron spectra of CI, CII, and CIII (split in CIIIa and CIIIb in Fig. 3). The attribution of CIIIa and CIIIb to the same magnetic near-surface phase and the exclusion of a reduction of the Néel temperature on top of this layer results unambiguously from the identical shape of both electron spectra. The depth distributions of CIIIa and CIIIb coincide. Figure 3 shows the development of the resonant electron spectra for three temperatures. At 323.25 K the electron spectra of CII and CIII are equal to the experimental response function, which means that the magnetic surface layer is too thin to result in a measurable energy loss of the electrons. Nevertheless, a thickness information is obtained by the absolute height of the signal, giving a much smaller thickness for CIII than for CII. The dominant contribution at this temperature comes from phase CI. The solid lines give the simulation results on the basis of the electron transport theory for the above three phase model. The stronger decrease with energy loss of the simulated bulk spectrum compared to experiment is due to transport properties that are seen only in single crystal spectra. They are considered to arise from electron channeling. In first order, this effect gives a systematic uncertainty for the depth deconvolution of 15% by a linear scaling factor for all depth values as it will affect the electron spectra at any temperature in the same way. Thus, the characteristic exponent for the temperature dependence of the surface layer thickness will not be affected.

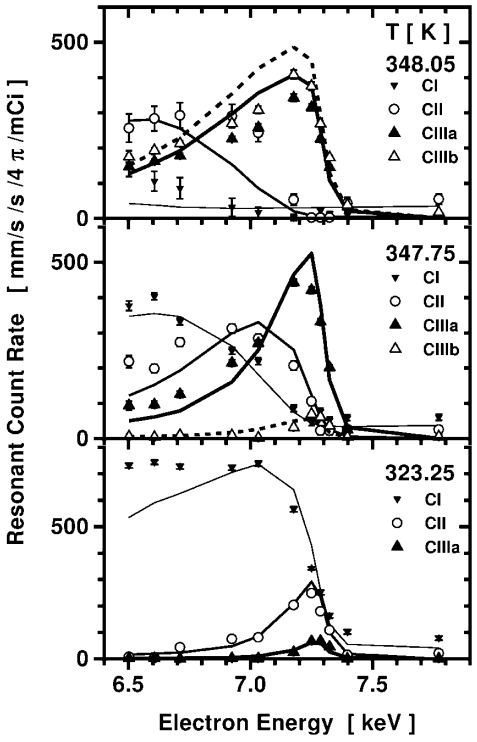

FIG. 3. Resonant count rate of components CI–CIII as a function of electron energy. With increasing temperature the intensity of the magnetic surface layer increases systematically.

At 347.75 K the electron spectra of CII and CIII are no longer similar. The edge of the spectrum of CII has shifted to a larger energy loss which equals the deeper region in the sample where this phase is found. Furthermore, the intensity of CIII has increased considerably which reflects the strong increase in volume. As the leading edge is unshifted this phase must still reach to the very surface. Already visible is a small contribution of the paramagnetic line CIIIb which becomes the dominant part at 348.05 K. At this higher temperature the similarity of the electron spectra of CIIIa and CIIIb becomes obvious. The contribution CI has nearly vanished and CII is found at even larger depths. The deviations in the shape of the simulated and experimental spectra for electron energies between 6.9 and 7.1 keV are due to the statistical correlation of CII and CIII in the Mössbauer spectra; thus CIII is slightly underestimated whereas CII is overestimated in intensity. Deviations in the absolute height are correlated with the already mentioned peculiarities of the electron transport in the single crystal.

The analysis of the resonant electron spectra for nine temperatures reveals the systematics of the volume variation of components CII and CIII with reduced temperature, or in a more direct way, with the magnetic hyperfine field B_{hf} of the bulk phase. For $B_{hf} \geq 10$ T, i.e., $t \geq 2$ K, the thickness DII and DIII follow a power law (Fig. 4). The multiplication of the exponent for DIII $\nu_3/\beta_1 = 1.7(1)$ by β_1 leads to the characteristic exponent $\nu_3 = 0.59(4)$. The temperature dependence of DII is much weaker and gives $\nu_2/\beta_1 = 0.5(1)$. Above 346.5 K the divergence is much stronger than the extrapolated power law. This coincides

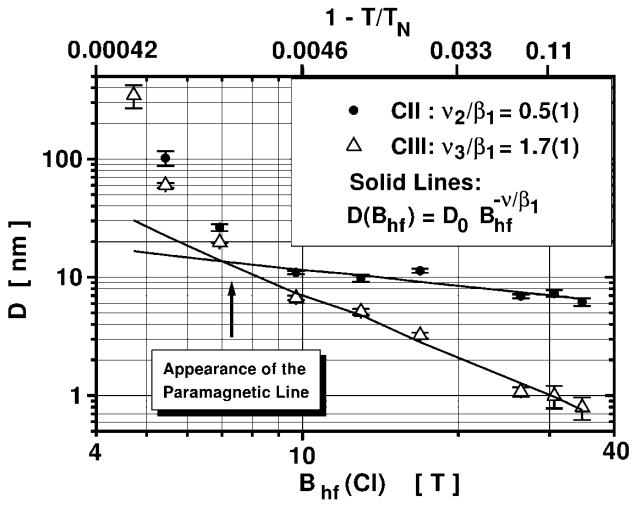

FIG. 4. Temperature dependence of the layer thickness DII and DIII. The deviation from the power law for $B_{hf} < 7$ T is significant, though the error bars get much larger as the Bethe range of the K conversion electrons is reached.

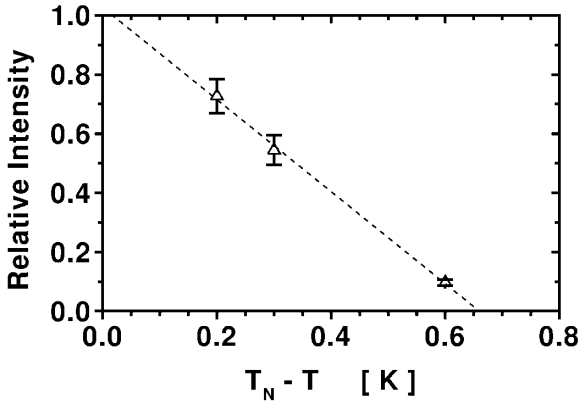

FIG. 5. Paramagnetic fraction CIIIb of component CIII.

with the appearance of the paramagnetic fraction of component CIII (Fig. 5).

By the DCEMS method the critical behavior of the volume fraction of a homogeneous magnetic near-surface phase of an antiferromagnetic $FeBO_3$ bulk single crystal could be observed over 2 orders of magnitude in thickness. Because of the depth resolution a phase boundary could be identified. The coexistence of the bulk and near-surface phase contradicts the theoretically proposed gradual dependence of the order parameter on depth in so-called ordinary or extraordinary transitions [14]. This finding will have significant implications on the interpretation of critical behavior in small particles. The characteristic exponent ν_3 for the thickness of the near-surface phase for $t \geq 2$ K is in striking agreement with the theoretical critical exponent $\nu_{\text{th}} = 0.63$ for the correlation length ξ_{bulk} in the three-dimensional Ising model [15–18]. The critical length scale ξ_{surface} for the surface of a semi-infinite system should be the same [14,19]. The exponent $\beta_3 = 0.51(2)$ lies between the bulk value and the surface value of the semi-infinite Heisenberg model [20–22] with $\beta = 0.8$. The similarity of ν_3 and ν_{th} is originated in the fact that both the increase of D and ξ with temperature is counteracted by the magnetocrystalline anisotropy. The effective dimensionality of the system seems to be 3. The steeper increase of D for $t < 1$ K hints to a reduction of this value. Parallel to the divergence of ξ for $t \rightarrow 0$ K, at $t = 0.65$ K a measurable fraction of the critical fluctuations reaches the Lamor precession time of the Mössbauer transition (10^{-8} s), which is seen in the paramagnetic contribution.

A. Kamzin expresses his gratitude to the Russian Fund for Fundamental Research (Grant No. 98-02-18279) for supporting this work. We are indebted to the continuous support of the Deutsche Forschungsgemeinschaft for the development of the DCEMS method.

[1] A. H. Morrish and K. Haneda, J. Magn. Magn. Mater. **35**, 105 (1983); T. Shinjo, Surf. Sci. Rep. **12**, 49 (1991); *Studies of Magnetic Properties of Fine Particles and their Relevance to Materials Science*, edited by J. L. Dormann and D. Fiorani (Elsevier Science Publishers B.V., New York/Amsterdam, 1992).
[2] U. Gradmann, Appl. Phys. **3**, 161 (1974); J. Magn. Magn. Mater. **100**, 481 (1991); S. Duncan *et al.*, Hyperfine Interact. **4**, 886 (1978); G. Bayreuther and G. Lugert, J. Magn. Magn. Mater. **35**, 50 (1983).
[3] A. M. van der Kraan, Phys. Status Solidi (a) **18**, 215 (1973).
[4] T. Shinjo *et al.*, J. Magn. Magn. Mater. **35**, 133 (1983).
[5] T. Yang *et al.*, Phys. Rev. Lett. **48**, 1292 (1982).
[6] L. Néel, J. Phys. Radium **15**, 225 (1954); M. I. Kaganov, Sov. Phys. JETP **61**, 1679 (1971); D. L. Mills, Phys. Rev. B **3**, 3887 (1971); T. Kaneyoshi, J. Phys. C **3**, 4497 (1991); A. J. Freeman and Ru-qian Wu, J. Magn. Magn. Mater. **100**, 497 (1991).
[7] B. Stahl and E. Kankeleit, Nucl. Instrum. Methods Phys. Res., Sect. B **122**, 149 (1997).
[8] G. N. Belozersky, *Mössbauer Studies of Surface Layers* (Elsevier, New York/Amsterdam, 1993); K. Nomura, Y. Ujihira, and A. Vertes, J. Radioanal. Nucl. Chem. Artic. **202**, 103 (1996).
[9] D. Liljequist, J. Phys. D **16**, 1567 (1983); **11**, 839 (1978).
[10] B. Stahl *et al.*, Hyperfine Interact. (to be published).
[11] A. Kamzin and L. A. Grigor'ev, Phys. Solid State **36**, 694 (1994).
[12] P. P. Kovalenko *et al.*, Sov. Phys. Solid State **29**, 340 (1987).
[13] M. Eibschütz, L. Pfeiffer, and J. W. Nielsen, J. Appl. Phys. **41**, 1276 (1970).
[14] H. Dosch, *Critical Phenomena at Surfaces and Interfaces: Evanescent X-Ray and Neutron Scattering*, Springer Tracts in Modern Physics Vol. 126 (Springer-Verlag, Berlin, 1992).
[15] G. S. Pawley *et al.*, Phys. Rev. B **29**, 4030 (1984).
[16] J. C. Le Guillou and J. Zinn-Justin, *Phase Transitions*, edited by M. Levy, J. C. Le Guillou, and J. Zinn-Justin (Plenum, New York, 1982).
[17] C. J. Hamer, J. Phys. A **16**, 1257 (1983).
[18] J. Adler, J. Phys. A **16**, 3585 (1983).
[19] K. Binder, *Phase Transitions and Critical Phenomena*, edited by C. Domb and J. L. Lebowitz (Academic Press, New York, 1983), Vol. 8.
[20] H. W. Diehl and S. Dietrich, Z. Phys. B **42**, 65 (1981); Z. Phys. B **43**, 315 (1981).
[21] K. Ohno, Y. Okabe, and A. Morita, Prog. Theor. Phys. **71**, 714 (1984).
[22] K. Binder and D. P. Landau, Phys. Rev. Lett. **52**, 318 (1984).